

# Stability Discriminant of a Tracked Vehicle to Traverse Stairs

Daisuke Endo

Tohoku University, endo@frl.mech.tohoku.ac.jp

Keiji Nagatani

Tohoku University, keiji@ieee.org

**Abstract**—In some surveillance missions in the aftermath of disasters, the use of a teleoperated tracked vehicle contributes to the safety of rescue crews. However, because of its insufficient traversal capability, the vehicle can become trapped upon encountering rough terrain. This may lead to mission failure and, in the worst case, loss of the vehicle. To improve the success rate of such missions, it is very important to assess the traversability of a tracked vehicle on rough terrains based on objective indicators. From this viewpoint, we first derived physical conditions that must be satisfied in the case of traversal on stairs, based on a simple mechanical model of a tracked vehicle. We then proposed a traversability assessment method for tracked vehicles on stairs. In other words, we established a method to evaluate whether or not a tracked vehicle can traverse the target stairs. To validate the method, we conducted experiments with an actual tracked vehicle on our mock-up stairs, and we observed some divergences between our calculation and the experimental result. Therefore, we analyzed possible factors causing these divergences, estimated the influence of the factors. In this paper, we report the above-described assessment method, the experiments, and the analyses.

## I. INTRODUCTION

Teleoperated small-sized tracked vehicles have two advantages compared to other vehicles: high traversability on rough terrain and a simple mechanism. Therefore, they are ideal for surveillance tasks to replace rescue crews in exploring hazardous environments in search and rescue missions. Well-known examples of tracked vehicles for practical use missions include Quince[1] and Survey Runner[2]. These robots explored the buildings affected by the meltdown of the Fukushima Daiichi nuclear power plant. These robots provided significant information during surveillance missions, particularly related to damage inspection of plants and acquisition of dose distribution. However, in their last missions, both tracked vehicles got stuck in rough terrain and could not return. To prevent such situations, various approaches have been proposed to improve the usability of tracked vehicles; these include semi-autonomous control of sub-tracks[3] and consideration of robot stability in path planning[4]. However, no fundamental study has been conducted on assessing the ability of a tracked vehicle to traverse rough terrains from the point of view of the interaction between the tracks and the ground, directly.

To improve the success rate of such surveillance missions, a prior assessment is crucial. For example, in the case of surveillance missions in buildings, tracked vehicles are required to traverse stairs for moving to another floor. However, stair-

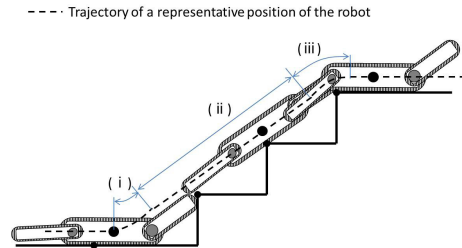


Fig. 1. Motion flow of a tracked vehicle traversing stairs.

climbing and stair-descending are obstacles that cause various problems in operation, and an assessment of traversability on stairs is important. Fig. 1 shows the motion flow for a tracked vehicle traversing stairs for the stair-climbing case. The motion flow is divided into three steps:

- (i) **Entering step:** the motion state from contacting the first step of the stairs to finishing its traversal (Fig. 1(i)).
- (ii) **Traversing step:** the intermediate state between (i) and (iii) (Fig. 1(ii)), in which the pitch angle of the robot matches the inclination angle of the stairs.
- (iii) **Landing step:** the motion state from contacting the final step of the stairs to finishing its traversal (Fig. 1(iii)).

In previous research, Guo et al. stated that, to ensure traversability of a tracked vehicle on stairs, initially, the first step should be clear[5]. However, they did not consider the situation after the second step of the stairs-traversal. Jingguo et al. conducted and examined a derivation of the physical condition to traverse stairs stably. However, they did not sufficiently validate its performance. Liu et al. proposed an online prediction system for monitoring the physical stability of a tracked vehicle [7]. However, no previous study has verified a physical model to predict the stability of a tracked vehicle on stairs.

In this light, we develop a method for assessing whether or not a tracked vehicle can traverse stairs. Among the three steps ((i)–(iii)) described above, in this research, we focus on the traversing step (ii), and we propose an assessment method to evaluate, in advance, whether or not a tracked vehicle can traverse stairs.

## II. PHYSICAL MODEL OF A TRACKED VEHICLE TRAVERSING STAIRS

### A. Failure modes of tracked vehicles traversing stairs

First, to model a stair traversal of a tracked vehicle, we classified failure modes of a tracked vehicle that may occur

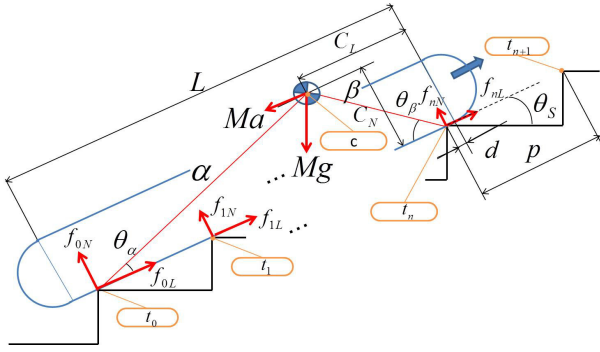


Fig. 2. Physical model of a tracked vehicle traversing stairs.

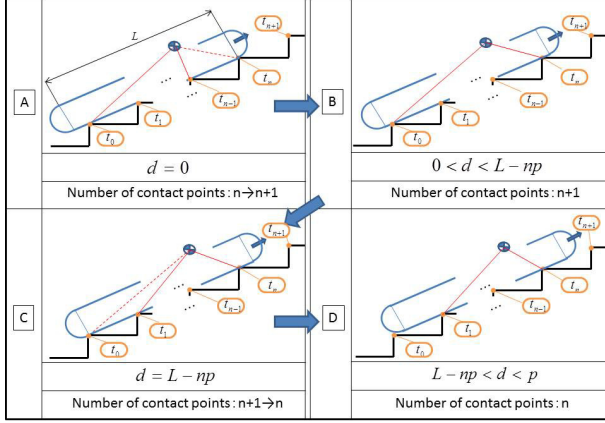


Fig. 3. State transitions of a tracked vehicle traversing stairs.

during its traversal on stairs, and we derived physical conditions that cause each failure mode. Fig. 2 shows a model of a tracked vehicle that has mass  $M$  in a two-dimensional plane as it traverses a flight of stairs. The angle of the stairs is  $\theta_s$ , and the distance between the leading edges of adjacent steps (pitch between the edges of the stairs) is  $p$ . The length of the flat area of the track is  $L$ , and it has  $n + 1$  (where  $n$  is an integer. This paper deals only with cases  $n \geq 2$ . Because in case  $n < 2$ , the tracked vehicle can not move on the stairs keeping the pitch angle match to the stairs.) contact points with the stairs. The contact points are defined as  $t_0, t_1, \dots, t_n$  from the bottom to the top. At each contact point, there are a tractive force  $f_{kL}$  and a vertical force  $f_{kN}$ . Here,  $k$  is an arbitrary integer between 0 and  $n$ . In addition, the robot is subject to an upward acceleration  $a$  along the stairs.

Fig. 3 shows the state transition of the tracked vehicle while it traverses target stairs. Transitions occur when the number of contact points changes. In Fig. 3, we assume  $np \leq L < (n + 1)p$ . The tracked vehicle traverses the stairs by transitioning through states  $A \rightarrow B \rightarrow C \rightarrow D \rightarrow A$ . When the track is in contact with the edge of a step, it is defined as state A. After that, it transitions to state B. When the track detaches from the edge of the step, it is defined as state C. After that, it transitions to state D.

To traverse the stairs successfully, a tracked vehicle should avoid the following three failure modes:

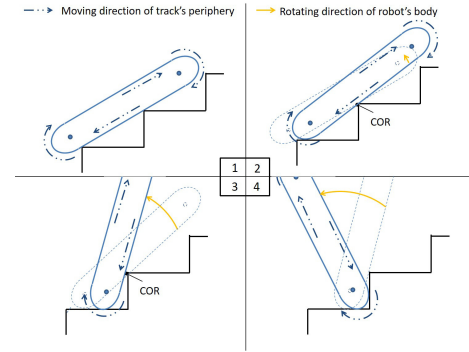


Fig. 4. Falling backward mode.

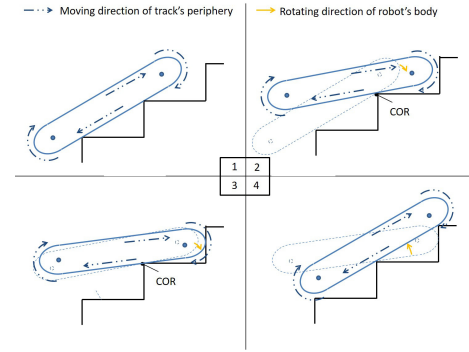


Fig. 5. Falling forward mode.

- 1) **Slipping:** the case in which the tractive force  $F_{kL}$  is insufficient, and the track slides down on the stairs.
- 2) **Falling backward:** the case in which the robot's body tips over around the center  $t_0$ , the direction of rotation being counterclockwise, as shown in Fig. 2.
- 3) **Falling forward:** the case in which the robot's body tips over around the center  $t_n$ , the direction of rotation being clockwise, as shown in Fig. 2.

The last mode (falling forward) occurs very rarely. It only occurs when the robot's centroid is located well forward in its body, and the robot is acted on by a large downward acceleration. In addition, this failure mode tends to cause less damage to the robot and its surrounding environment than the falling-backward mode.

This paper addresses and describes the physical conditions required to prevent the occurrence of these failure modes.

### B. Slipping

When the traction force generated at the contact points between the tracks and the stairs does not exceed the static friction force, the tracked vehicle traverses the stairs without slipping. The condition is expressed by

$$\sum_{k=0}^n f_{kL} < \mu_S \sum_{k=0}^n f_{kN}, \quad (1)$$

where  $f_{kL}$  and  $f_{kN}$  are the tractive force and normal reaction force, respectively, at contact point  $t_k$  (where  $k$  is an arbitrary

integer between 0 and  $n$ ) and  $\mu_S$  is the coefficient of friction between the tracks and the stairs. In this paper, it is assumed that  $\mu_S$  has the same value at each contact point.

The equilibria of the lateral and longitudinal forces that describe the condition at which the robot is prevented from slipping can be expressed as

$$Ma = \sum_{k=0}^n f_{kL} - Mg \sin \theta_s, \quad (2)$$

$$0 = \sum_{k=0}^n f_{kN} - Mg \cos \theta_s, \quad (3)$$

where  $M$  is the mass of the tracked vehicle,  $a$  is the lateral acceleration of the tracked vehicle,  $g$  is the gravitational acceleration, and  $\theta_s$  is the angle of inclination of the stairs. Substituting Equations (2) and (3) into Equation (1) and rearranging to obtain acceleration  $a$  gives

$$\begin{aligned} Ma + Mg \sin \theta_s &< \mu_s Mg \cos \theta_s. \\ \therefore a &< (\mu_s \cos \theta_s - \sin \theta_s)g. \end{aligned} \quad (4)$$

### C. Falling backward

For a tracked vehicle to successfully traverse stairs, the summation of its angular moments must be zero. When a tracked vehicle has  $n+1$  contact points without any rotation, as shown in Fig. 2, the balance of its moment around point  $t_0$  can be described as follows:

$$\sum_{k=1}^n kp f_{kN} + Ma\alpha \sin \theta_\alpha - Mg\alpha \cos(\theta_s + \theta_\alpha) = 0, \quad (5)$$

where  $\alpha$  is the distance between the centroid  $C$  and the contact point  $t_0$ , and  $\theta_\alpha$  is the angle formed by  $t_n$  and  $t_0$  and  $C$  ( $\angle t_n t_0 C$ ). When the robot rotates around the point  $t_0$ , there are no other contact points. Therefore, in this case,  $f_{kN}$  is equal to 0 (where  $k$  is an arbitrary integer between 1 and  $n$ ) in Equation (5), and the left-hand side of this formula becomes greater than 0. Thus, we can derive

$$\begin{aligned} Ma\alpha \sin \theta_\alpha - Mg\alpha \cos(\theta_s + \theta_\alpha) &> 0, \\ a &> \frac{\cos(\theta_s + \theta_\alpha)}{\sin \theta_\alpha} g. \\ \therefore a &> \left( \frac{\cos \theta_s}{\tan \theta_\alpha} - \sin \theta_s \right) g. \end{aligned} \quad (6)$$

The complementary condition to that described by Equation (6) is required to prevent the robot from falling backward. Therefore, we derive

$$a \leq \left( \frac{\cos \theta_s}{\tan \theta_\alpha} - \sin \theta_s \right) g. \quad (7)$$

With regard to  $\triangle t_0 t_n C$ ,  $\theta_\alpha$  in Equation (7) should satisfy

$$\theta_\alpha = \arccos \left( \frac{\alpha^2 + n^2 p^2 - \beta^2}{2n\alpha p} \right), \quad (8)$$

$$\alpha = \sqrt{(d + np - C_L)^2 + C_N^2}, \quad (9)$$

$$\beta = \sqrt{(C_L - d)^2 + C_N^2}, \quad (10)$$

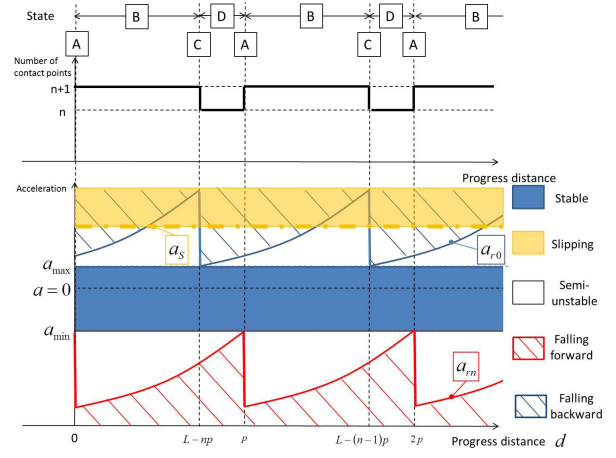


Fig. 6. Stability profile of a tracked vehicle traversing stairs.

where  $\alpha$  is the distance between centroid  $C$  and contact point  $t_0$ ;  $\beta$  is the distance between centroid  $C$  and contact point  $t_n$ ;  $d$  is the robot's progress, which is equal to 0 at state A in Fig. 3;  $C_L$  is the distance between the tip in the flat area of the track and the centroid  $C$  in the front-back direction; and  $C_N$  is the distance between the bottom of the track and the centroid  $C$  in the up-down direction.

### D. Falling forward

In the falling-backward mode, when a tracked vehicle has  $n+1$  contact points without any rotation, as shown in Fig. 2, the balance of its moments around point  $t_n$  can be described as follows:

$$\begin{aligned} \sum_{k=0}^{n-1} (n-k)p f_{kN} - Ma\beta \sin \theta_\beta \\ - Mg\beta \cos(\theta_\beta - \theta_s) = 0. \end{aligned} \quad (11)$$

In the case of falling backward, the requirement to prevent the robot from falling forward is derived from

$$a \geq - \left( \frac{\cos \theta_s}{\tan \theta_\beta} + \sin \theta_s \right) g, \quad (12)$$

where  $\theta_\beta$  is  $\angle t_0 t_n C$ . With regard to  $\triangle t_0 t_n C$ ,  $\theta_\beta$  is described by

$$\theta_\beta = \arccos \left( \frac{\beta^2 + n^2 p^2 - \alpha^2}{2n\beta p} \right). \quad (13)$$

## III. TRAVERSING ABILITY ASSESSMENT METHOD

Fig. 6 shows a schematic diagram of the  $d$ - $a$  plane. The vertical axis indicates the acceleration  $a$  of the robot, and the horizontal axis indicates the distance  $d$  that the robot progresses. The diagram includes (a) the state transition as a tracked vehicle traverses a flight of stairs and (b) the requirements for acceleration to prevent the robot from entering the failure modes described above. Furthermore,  $a_s$ ,  $a_{r0}$ , and  $a_{rn}$  are the marginal accelerations required to prevent the

vehicle from slipping, falling backward, and falling forward, respectively. They are defined by

$$a_S = (\mu_s \cos \theta_s - \sin \theta_s)g, \quad (14)$$

$$a_{r0} = \left( \frac{\cos \theta_s}{\tan \theta_\alpha} - \sin \theta_s \right) g, \quad (15)$$

$$a_{rn} = - \left( \frac{\cos \theta_s}{\tan \theta_\beta} + \sin \theta_s \right) g. \quad (16)$$

These equations imply that slipping occurs when the acceleration of the robot is greater than  $a_S$ , falling backward occurs when the acceleration of the robot is greater than  $a_{r0}$ , and falling forward occurs when the acceleration of the robot is less than  $a_{rn}$ . Here,  $a_{max}$  is defined as the lesser of the value of  $a_S$  and the minimum value attained by  $a_{r0}$ , and  $a_{min}$  is the maximum value attained by  $a_{rn}$ , as expressed, respectively, by

$$a_{max} = \min(a_S, \min(a_{r0})), \quad (17)$$

$$a_{min} = \max(a_{rn}). \quad (18)$$

The stability can be assessed based on the schematic diagram shown in Fig. 6. The  $d$ - $a$  plane is divided into the following five areas, and the robot's stability can be categorized into one of the following states:

- A) **Slipping area:** When the acceleration  $a$  does not satisfy Equation (4), the robot's body slips along the flight of stairs.
- B) **Falling-backward area:** When the acceleration  $a$  satisfies Equation (4) but does not satisfy Equation (7), the robot's body rotates around the contact point  $t_0$ .
- C) **Falling-forward area:** When the acceleration  $a$  does not satisfy Equation (12), the robot's body rotates around the contact point  $t_n$ .
- D) **Stable area:** When the acceleration of the robot satisfies the condition  $a_{min} < a < a_{max}$ , it can traverse stairs without any slipping or rotation.
- E) **Semi-unstable area:** This area cannot be categorized as any of (A)–(D) above; however, it satisfies Equations (7) and (12). The robot can traverse the stairs.

The robot needs to be controlled to maintain its acceleration  $a$  in the semi-unstable area, according to the robot's position on the stairs. If the robot cannot control its acceleration accurately according to its position on the stairs, this area should be considered unstable. In this case, the robot should be controlled in the stable area (D). Additionally, note that the robot slips prior to rotation if the acceleration  $a$  does not satisfy Equations (4) and (7).

In other words, the robot can traverse the stairs without any slipping or rotation if its acceleration is controlled in the stable area (D).

#### IV. CASE STUDY

We conducted a case study with a tracked vehicle, called "Kenaf"[8], that traverses stairs using the traversability assessment method described in the previous section. In this case study, we assumed that the robot's speed was constant

(acceleration  $a = 0$ ). There were two reasons for this assumption. One is because it is difficult for Kenaf to maintain its acceleration when moving on stairs owing to the power restriction of its actuators. The other is that the increase and decrease in acceleration are equivalent to that of the inclination of stairs based on the physical model shown in Fig. 2. In addition, Kenaf originally has two main tracks and four sub-tracks. However, to improve the accuracy of the verification tests described in the next section, the robot's mechanical system should be simple. Therefore, we used Kenaf without all of its sub-tracks; only the two main tracks were used in this case study (Fig. 7). The physical parameters of the robot, as used for the calculation, are listed in Table I.

Kenaf has multiple convex-shaped grousers made of chloroprene rubber on the surface of the tracks. Therefore, the friction between the tracks and the ground is sufficient to prevent slipping, and falling backward occurs prior to slipping on stairs with large inclinations in the preliminary experiments. In other words, in case of  $a_S > \min(a_{r0})$ , slipping does not occur. Furthermore, falling forward did not occur at constant speed. Consequently, we only consider the falling-backward phenomenon for assessing problems related to the shape of the stairs for Kenaf.

The shape of the stairs can be described by two parameters: the angle of inclination of the stairs,  $\theta_s$ , and the pitch between the edges of the stairs,  $p$ . The condition for whether falling backward occurs (described as "margin" in this paper) in the  $\theta_s$ - $p$  plane can be derived by substituting  $a = 0$  in Equations (7)–(10). This margin can be described by the following set of equations:

$$\theta_s^{sup} = \frac{\pi}{2} - \theta_{\alpha C}, \quad (19)$$

$$\theta_{\alpha C} = \arccos \left( \frac{\alpha_C^2 + (n-1)^2 p^2 - \beta_C^2}{2(n-1)\alpha_C p} \right), \quad (20)$$

$$\alpha_C = \sqrt{\{d_C + (n-1)p - C_L\}^2 + C_N^2}, \quad (21)$$

$$\beta_C = \sqrt{(C_L - d_C)^2 + C_N^2}, \quad (22)$$

$$d_C = L - np. \quad (23)$$

The solid line in Fig. 9 shows the predicted margin obtained by substituting Kenaf's parameters (Table I) into Equations (19)–(23). This means that, theoretically, the robot falls backward in the area on the right, but not in the area on the left in the plane bounded by the solid line.

TABLE I  
ROBOT SPECIFICATIONS.

Parameter	Symbol	Value
Centroid position in front-back direction	$C_L$	196 [mm]
Centroid position in up-down direction	$C_N$	71 [mm]
Length of flat area	$L$	470 [mm]

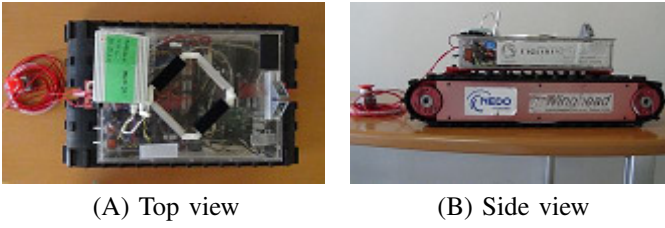


Fig. 7. The target tracked vehicle used in our verification test.



Fig. 8. Changeable mock-up stairs

## V. VERIFICATION TEST

To verify the traversability assessment method, we conducted verification tests to compare with the predicted margin obtained in the previous section.

### A. Equipment

For this test, we used Kenaf (Fig. 7). Besides, we fabricated the mock-up stairs shown in Fig. 8. The setup allowed us to change the inclination  $\theta_s$  of the stairs to any value between  $0^\circ$  and  $70^\circ$ , and the pitch between the edges of the stairs,  $p$ , could be changed to any value.

### B. Test procedure

We conducted traversal tests under different  $(\theta_s, p)$  conditions. For each trial, the tracked vehicle was placed on the mock-up stairs and operated to climb up vertically to the end of the stairs at a constant speed, 100 mm/s (acceleration  $a = 0$ ). We then observed its behavior and judged whether or not falling backward occurred. At the tip of the robot, a safety tether was attached to prevent the robot from falling and crashing. The pitch between the edges of the stairs,  $p$ , was changed to four different values—150, 180, 200, and 220 mm—and the inclination of the stairs  $\theta_s$  was changed discretely. At each pitch between the edges of the stairs, we evaluated the marginal inclination  $\theta_s^{sup}$  above which falling backward occurred. We performed five trials under the same conditions.

## VI. TEST RESULTS AND DISCUSSION

Fig. 9 shows the results of the above tests. These are in good agreement with the predicted values in those areas where the inclination  $\theta_s$  is relatively small. These results indicate that

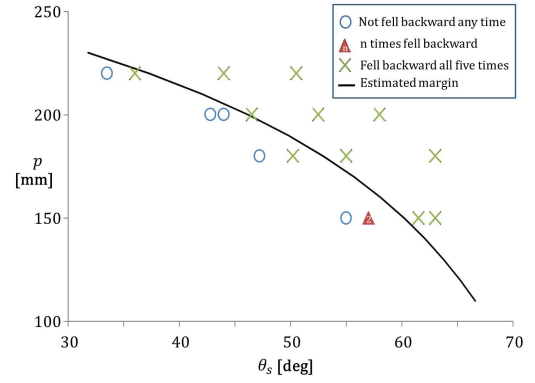


Fig. 9. Experimental results.

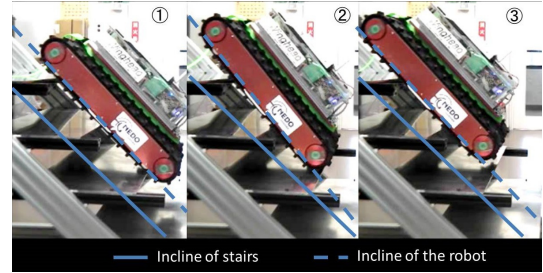


Fig. 10. Robot's behavior when traversing stairs ( $\theta_s = 44.0^\circ$ ,  $p = 200$  mm).

the falling-backward phenomenon predominantly depends on the relation between the robot's centroid and the shape of the stairs, as described in Equations (19)–(23). However, in those areas where  $\theta_s$  is large, the predicted values diverged from the measured values. The largest difference was observed when  $p = 150$  mm: the robot fell down at  $55.0^\circ$ – $57.0^\circ$  in the experiment; however, the predicted margin was  $60.2^\circ$ . Fig. 10 shows the behavior of the robot when the robot traverses a flight of stairs for which  $\theta_s = 44.0^\circ$  and  $p = 200$  mm. The falling-backward phenomenon did not occur in this case; however, the robot's body started to exhibit a swinging motion, as shown in Fig. 10(2). This situation occurred when the edge of the track detached from the contact point. Moreover, the robot satisfies Equation (7) at this instant, because the projecting point of the robot's centroid is located within the polygon formed from the contact points without a detaching point. Therefore, the other phenomenon must have occurred exactly when the edge of the track detached. In the next section, we discuss the reasons for this divergence.

### A. Deformation of the track

Generally, a tracked vehicle, including Kenaf, has multiple grousers across the surface of its tracks to increase the friction between the track's surface and the ground, thereby preventing the track from slipping. Typically, for small tracked vehicles, the tracks are made of a nonrigid material. Therefore, bending deformation of the track occurs at the point where the grouser comes into contact with the edge of the stairs, particularly at the lowermost contact point. As a result, the deformation

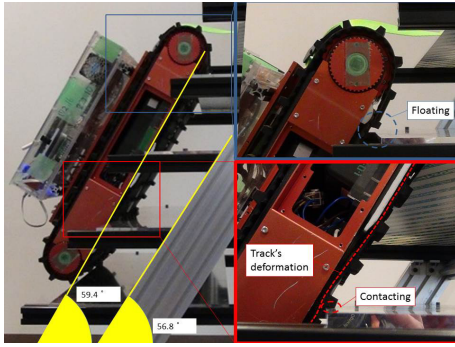


Fig. 11. Increase of the pitch angle of the robot caused by track deformation.

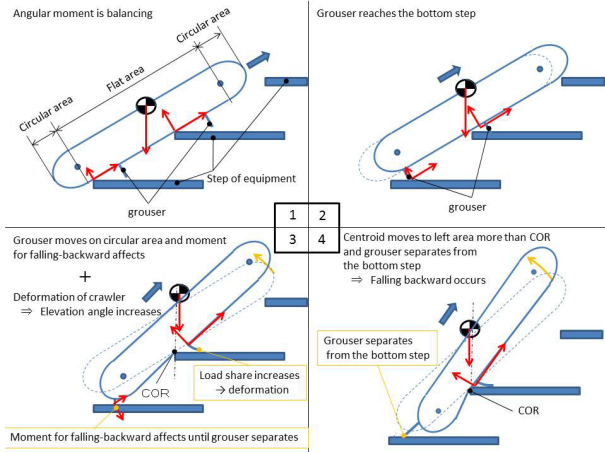


Fig. 12. Falling-backward mode affected by track deformation and rib.

increases the pitch angle of the robot's body. When the load-sharing ratio at the bottom of the contact point is maximized, the pitch angle of the body is also maximized, as shown in Fig. 11. Fig. 11 shows a side view of the robot's state on stairs with  $(p, \theta_s) = (150 \text{ mm}, 56.8^\circ)$ . In this case, the result was  $2.6^\circ$  greater than the inclination angle of the stairs.

### B. Lowest contact point angular moment generation by grousers

When the lowermost contact point of a track detached from the edge of a step, it takes some time because of the action of the grouser. During this period, the grouser causes the circular part of the track to move, and it generates an angular moment that pushes the lower part of the robot's body down, as shown in Fig. 12(3). The moment at the lowest contact point angular moment is abbreviated as LCM in this paper. This period is very short, but it increases the pitch angle of the robot's body. When the robot is just about to tip over, the LCM may provide the impetus for the robot to fall backward.

## VII. CONCLUSION AND FUTURE WORK

Based on a mechanical model, we have derived the physical conditions under which a tracked vehicle can traverse stairs without falling, and we have performed verification tests using

a tracked vehicle to clarify the backward-falling failure mode. As a result, for stairs with relatively small inclination, it is possible to assess whether they can be traversed by the robot based on the robot's centroid, the length of track, inclination, and the pitch between the edges of the stairs. However, for stairs with very large inclination, we confirmed that the robot fell backward more easily than indicated by our calculations. Therefore, we discussed about this error, and estimated that there are two primary factors for the robot to tip: the deformation of the tracks caused by the increase of load sharing at the lowermost contact point and the influence of the LCM generated by the grouser that maintains contact when it moves along the circular part of the track.

In near future work, we will evaluate the influence of each primary factor quantitatively by additional experiments. It can be expected that the accuracy of the assessment improves by our work not only on the stairs but also on general terrains whose inclination and pitch between contact points are not constant.

## ACKNOWLEDGEMENTS

This work was supported in part by a Grant-in-Aid for JSPS Fellows (No. 16J2554). Also, we gratefully acknowledge the work of past and present members of our laboratory, especially, Mr. Kai Kudo, contributing to some interpretation of data.

## REFERENCES

- [1] Tomoaki Yoshida, Keiji Nagatani, Satoshi Tadokoro, Takeshi Nishimura, and Eiji Koyanagi. Improvements to the rescue robot Quince toward future indoor surveillance missions in the Fukushima Daiichi Nuclear Power Plant. Preprints of the 8th International Conference on Field and Service Robotics, #80, 2012.
- [2] Tokyo Electric Power Co., Inc. Guide to citing Internet sources. [cited 2012 Mar 1]. Available from: [http://www.tepco.co.jp/en/nu/fukushima-np/images/handouts\\_120417\\_03-e.pdf](http://www.tepco.co.jp/en/nu/fukushima-np/images/handouts_120417_03-e.pdf)
- [3] Yoshito Okada, Keiji Nagatani, Kazuya Yoshida, Tomoaki Yoshida, and Eiji Koyanagi. Shared autonomy system for tracked vehicles to traverse rough terrain based on continuous three-dimensional terrain scanning. Proceedings of the 2010 IEEE/RSJ International Conference on Intelligent Robots and Systems, pages 357–362, 2010.
- [4] Evgeni Magid, Takashi Tsubouchi, Eiji Koyanagi, and Tomoaki Yoshida. Static balance for rescue robot navigation: Losing balance on purpose within random step environment. Proceedings of the 2010 IEEE/RSJ International Conference on Intelligent Robots and Systems, pages 349–356, 2010.
- [5] Y. Guo, A. Song, J. Bao, H. Zhang, and H. Tang. Research on centroid position for stairs climbing stability of search and rescue robot. International Journal of Advanced Robotic Systems, Vol. 7, No.4, pages 24–30, 2010.
- [6] Jingguo Liu, Yuechao Wang, Shungen Ma, and Bin Li. Analysis of stairs-climbing ability for a tracked reconfigurable modular robot. Proceedings of the 2005 IEEE International Workshop on Safety, Security and Rescue Robotics, pages 36–40, 2005.
- [7] Yungang Liu and Guangjun Liu. Track-stair interaction analysis and online tipover prediction for a self-reconfigurable tracked mobile robot climbing stairs. IEEE/ASE Transactions on Mechatronics, Vol. 14, No. 5, pages 528–538, 2009.
- [8] Tomoaki Yoshida, Eiji Koyanagi, Satoshi Tadokoro, Kazuya Yoshida, Keiji Nagatani, Kazuhro Ohno, Takashi Tsubouchi, Shoichi Maeyama, Itsuki Noda, Osamu Takizawa, and Yasushi Hada. A high mobility 6-crawler mobile Robot "Kenaf." Proceedings of the 4th International Workshop on Synthetic Simulation and Robotics to Mitigate Earthquake Disaster, page 38, 2007.